40. PV-Symposium 2025

Conference papers

https://doi.org/10.52825/pv-symposium.v2i.2687

Published: 27 Aug. 2025

Topcon Solar Modules

UV Degradation in Lab and Field Conditions

Sandra Lust[1,*], Shiva Ram Kuntamukkula[1], Sören Friedrichs[2], and Lars Podlowski[2]

[1]Kiwa PI Berlin AG, Germany

[2]SOLYCO Solar AG, Germany

*Correspondence: Sandra Lust, lust@berlin.de

Abstract. The UV degradation of TOPCon solar modules with different material compositions (BOM) was investigated and correlated in both field studies and accelerated aging laboratory tests. A UV treatment with 120 kWh/m² leads to significant power losses ranging from 1.3% to 13.7%, indicating a strong dependence on the specific material composition. Furthermore, it was found that additional degradation occurs beyond 120 kWh/m². Electroluminescence images (EL images) of laboratory UV-degraded modules show a characteristic checkerboard pattern indicative of UV-induced degradation (UVID). Additional degradation occurred during storage, which was partially reversible when the modules were re-irradiated.

After nine months in a ground-mounted system in Forst/Brandenburg, power losses of up to 2.4% were detected. Notably, this degradation was slightly lower than expected from UV-induced degradation tests (UVID) conducted in the laboratory. The EL images of field modules also displayed the characteristic checkerboard pattern, indicating that the UV degradation measured in the laboratory poses a real risk to the long-term stability of TOPCon modules in the field.

Due to the small number of modules examined, the statistical significance of the study is limited. Nevertheless, the results provide evidence of UV degradation of TOPCon modules under field conditions.

Keywords: TOPCon, Solarmodule, UV-Degradation

1. Introduction

Recent studies have focused on the ultraviolet (UV) degradation of TOPCon solar modules, a critical factor affecting their long-term stability. The degradation is primarily attributed to damage to the front-side passivation of the solar cells, which is influenced by several manufacturing process steps [1-5]. Key factors include the thickness, quality, and homogeneity of the aluminum oxide/silicon nitride double layer, as well as the doping profile of the emitter [6,7]. These parameters can vary in industrial production, leading to potential quality fluctuations even among modules that pass certification tests.

Despite the importance of understanding UV degradation, the extent of its impact under real-world field conditions remains uncertain. This study aims to bridge this knowledge gap by comparing laboratory UV tests with field exposure results for TOPCon modules. By examining the performance of modules with different material compositions under both controlled laboratory conditions and real-world outdoor exposure, this research provides insights into the actual risks and mitigation strategies for UV-induced degradation in TOPCon solar modules.

2. Material and methods

Nine commercial, bifacial TOPCon solar modules from eight different manufacturers were investigated. These modules, designated as types A to I, are based on nine different Bills of Materials (BOMs) and offer a variety of technical specifications and performance characteristics.

To correlate the UV degradation of TOPCon modules with different BOMs in the field and in the laboratory, solar modules from eight different manufacturers with nine different BOMs (module types A - I) were initially irradiated in short-circuit mode in the UV chamber with 120 kWh / m² of UV light. The chamber temperature was maintained at a constant 60°C. Before treatment and after each exposure of 15, 30, 60, 90, and 120 kWh / m², the IV characteristics of the modules were determined, and electroluminescence images were captured. The test sequence is shown in Figure 1 on the left.

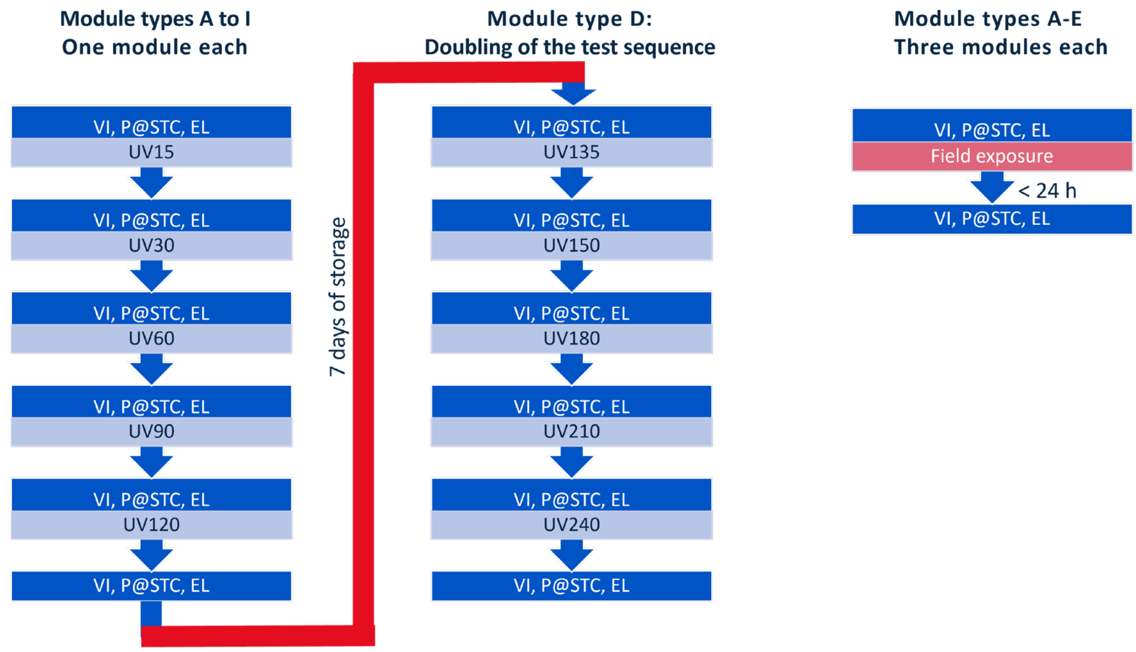

Figure 1. *First UV test sequence (left), enhanced UV test sequence (middle), field exposure test (right).*

The power measurements were conducted using a module flasher P@STC, with the Pasan SS3b being employed. These measurements were performed in accordance with the standards IEC 61215-2:2021-02 MQT 06 and IEC 60904-1:2020-09. The reproducibility of the measurements for the maximum power output Pmpp, open-circuit voltage Voc, and short-circuit current Isc was ± 0.6 % each.

Before every power mesurement, a visual inspection was performed according to IEC 61215-2:2021-02 MQT 01 to detect any visual defects in the module, such as cracked or broken cells, discoloration of the encapsulant, bubbles, delamination, or any other conditions that may affect module performance.

The accelerated UV aging tests were conducted by irradiating the front side of the modules while the back side was covered. The tests were performed in short-circuit mode. The UV chamber complied with the specifications of the standards IEC 61215-2:2021-02 MQT 10 and

IEC 61730-2:2016-08 MST 54. The UV spectrum consisted of a ratio of UV-A (320-400 nm) of 90 – 97 % and UV-B (280-320 nm) of 3 – 10 %. The module temperature was set at (60 ± 5) °C, and the irradiance was limited to less than 250 W / m². The lamp spectrum is shown in Figure 2.

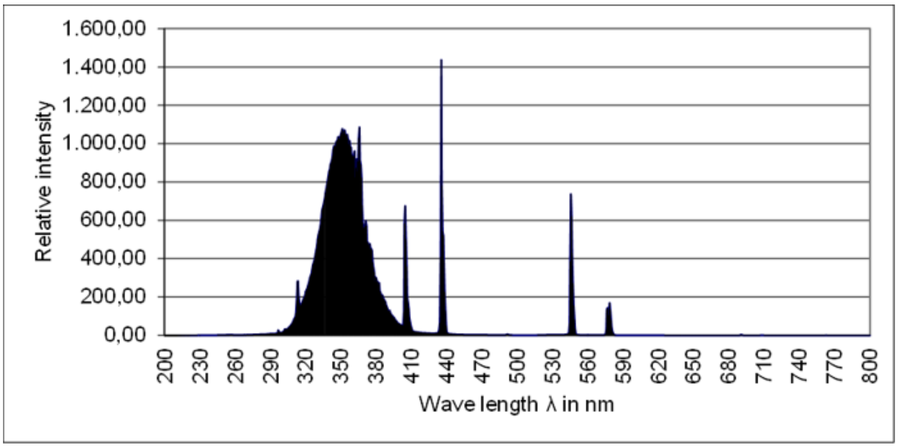

Figure 2. *UV lamp spectrum.*

For electroluminescence analysis is performed according to Kiwa PI Berlin internal specifications. A current in the range of the ISC is applied in forward direction, resulting in a radiation of the cells of the PV module in the infrared range. Performance measurements and EL images of the modules were taken within 24 hours after the end of the UV test.

In the solar installation in Forst, Brandenburg, fifteen TOPCon solar modules (three modules each of the five module types A-E) were installed from November 2023 to September 2024 with a 30° tilt facing south (182°). Each solar module was equipped with its own inverter. The back sides of the bifacial modules were sealed to prevent illumination of the back side. For the field modules, performance measurements and EL images were also taken within 24 hours after disassembly of the modules. To estimate the UV dose of the field modules, NASA data on UV radiation for the site were used. Due to the lack of current data, the previous year's data were utilized for the period from August 1 to September 11, 2024. According to this, the UV radiation over the nine months was approximately 55 kWh/m², and considering the tilt, it was about 68 kWh/m².

3. Results

Initial power measurements show a discrepancy between the labeled and actual measured power which highlights the importance of individual module measurements prior to exposure, as can be seen in table1.

Table 1. *Labelled and actual measured power Pmpp of modules used for UVID testing.*

Module		Pmpp [W]	Δ Pmpp [%]
A	Label	420	-0,36
	KIWA PI	418,5	
B	Label	425	-0,24
	KIWA PI	424	
C	Label	430	-4,37
	KIWA PI	411,2	
D	Label	k.A.	
	KIWA PI	430,9	
E	Label	400	2,17
	KIWA PI	408,7	
F	Label	450	-1,60
	KIWA PI	442,8	
G	Label	420	-3,55
	KIWA PI	405,1	
H	Label	k.A.	
	KIWA PI	403,9	
I	Label	420	-5,19
	KIWA PI	398,2	

3.1 Accelerated UV aging tests

Figure 3 shows the loss of maximum power (Pmpp), open-circuit voltage (ΔVoc), short-circuit current (ΔIsc), and fill factor (ΔFF) for the TOPCon modules A-I as a function of UV irradiation dose. The power loss increases continuously with rising UV dose. At an irradiation dose of 120 kWh/m², the loss reaches up to 14%, with modules exhibiting varying rates of decline. This decline in performance is primarily attributed to a significant decrease in open-circuit voltage, and short-circuit current. The fill factor remains largely constant across the entire UV dose range (except for Module I with ΔFF = 1.36% at 120 kWh/m²). These findings are consistent with similar measurements reported in recent publications ([2-5]).

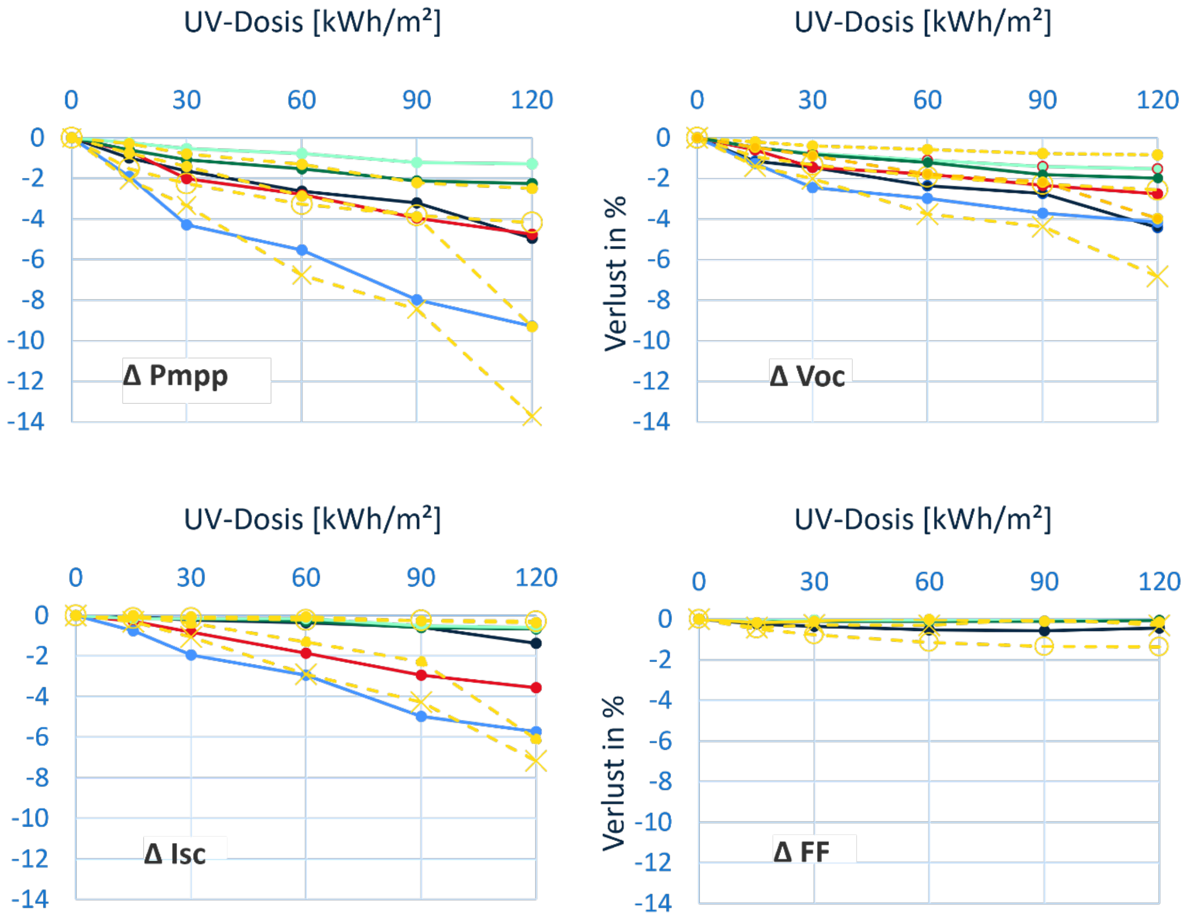

Figure 3. *Loss of maximum power (Pmpp), open-circuit voltage (ΔVoc), short-circuit current (ΔIsc), and fill factor (ΔFF) for the TOPCon modules A-I as a function of UV irradiation dose.*

Figure 4 illustrates the degradation behavior of Module D of subsequent UV exposure up to 240 kWh/m² (UV 240). The module exhibits a progressive decline in performance and reaches a power loss (ΔPmpp) of 4.9% at a dose of 120 kWh/m² (UV120), accompanied by reductions in open-circuit voltage (ΔVoc) and short-circuit current (ΔIsc). The fill factor (ΔFFΔFF) remains stable throughout the exposure. After UV120 exposure, the module was stored in darkness for seven days. During this period, further degradation occurred, with the maximum power loss increasing from 4.9% to 6.7%. This suggests that UV-induced damage may continue to propagate even in the absence of active irradiation, likely due to material relaxation or delayed chemical reactions. Interestingly, subsequent UV irradiation appears to partially "heal" the degradation observed during dark storage. This phenomenon indicates potential recovery mechanisms activated by further UV exposure, such as annealing effects or stabilization of defect states. Beyond UV120, the degradation initially stagnates before resuming at higher doses. By UV240, the maximum power loss reaches 8.3%, indicating that prolonged exposure exacerbates performance decline despite intermittent recovery phases.

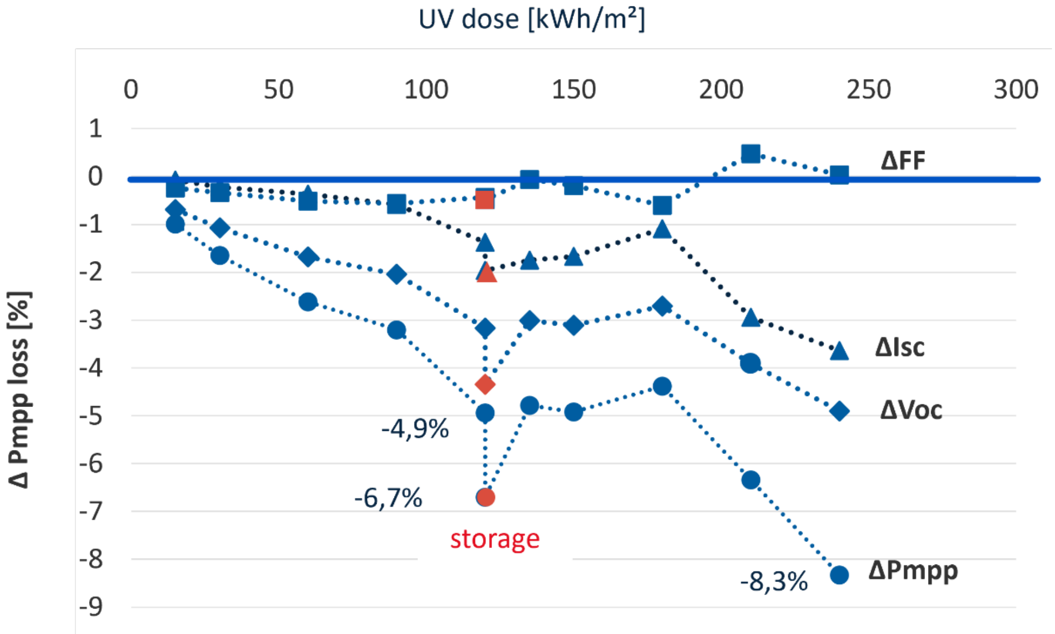

Figure 4. *UVID of Module D under subsequent UV exposure up to 240 kWh/m² and intermediate dark storage...*

The graph demonstrates that Module D undergoes significant performance losses under UV exposure, with additional degradation during dark storage suggesting complex material dynamics. While further UV irradiation can induce partial recovery, prolonged exposure ultimately leads to increased degradation. These findings highlight the importance of understanding both immediate and delayed effects of UV exposure on photovoltaic module performance.

Figure 5 shows the electroluminescence (EL) images of Module D. These images correspond to the measurement points in the previous graph (Figure 4), where performance losses such as ΔPmpp, ΔVoc, ΔIsc, and ΔFF were analyzed.

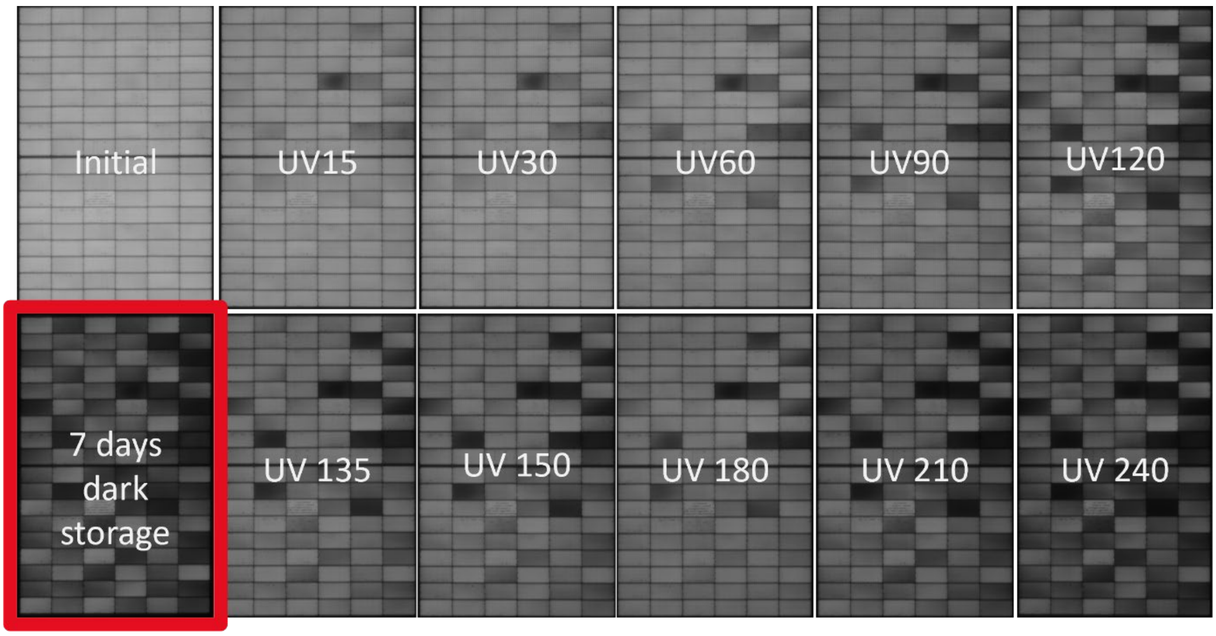

Figure 5. *Electroluminescence (EL) images of Module D under UV exposure.*

The initial EL image shows a uniform brightness across the module, indicating consistent electrical activity. As UV exposure progresses (UV15 to UV90), localized dark areas begin to appear, corresponding to regions of reduced electrical activity or degradation. These changes are likely due to UV-induced material damage. By UV120, the EL image reveals more pronounced dark areas, indicating further degradation. This corresponds to the measured drop in ΔPmpp and ΔVoc in Figure 4. The degradation is spatially heterogeneous, suggesting that certain regions of the module are more susceptible to UV-induced damage.

After seven days of dark storage following UV120 exposure, the EL image shows an increase in darkened areas compared to UV120. This aligns with the observed additional performance loss during storage (ΔPmpp drop from -4.9% to -6.7%). The continued degradation during storage may result from delayed chemical reactions or relaxation processes within the module materials.

Following dark storage, subsequent UV exposure leads to partial recovery in some regions, visible as slightly brighter areas in EL images at UV135 and UV150. However, prolonged exposure beyond UV150 results in further degradation, with extensive darkening by UV240. This corresponds to the stagnation and eventual worsening of performance parameters seen in Figure 4 (ΔPmpp reaching -8.3%).

The EL images provide visual confirmation of the degradation mechanisms observed in Figure 4. They highlight spatially heterogeneous damage caused by UV irradiation and its progression during dark storage. Partial recovery during subsequent UV exposure suggests complex dynamic processes within the module materials, such as defect annealing or stabilization, followed by renewed deterioration under prolonged stress conditions.

3.2 Outdoor exposure

Figure 6 display the average changes in key performance parameters—maximum power (ΔPmpp), open-circuit voltage (ΔVoc), short-circuit current (ΔIsc), and fill factor (ΔFF)—for five module types (A, B, C, D, E) after outdoor exposure from November 2023 to September 2024 in Forst, Brandenburg. Each data point represents the mean of three measurements from three modules per type, with error bars indicating the variation among the individual module values.

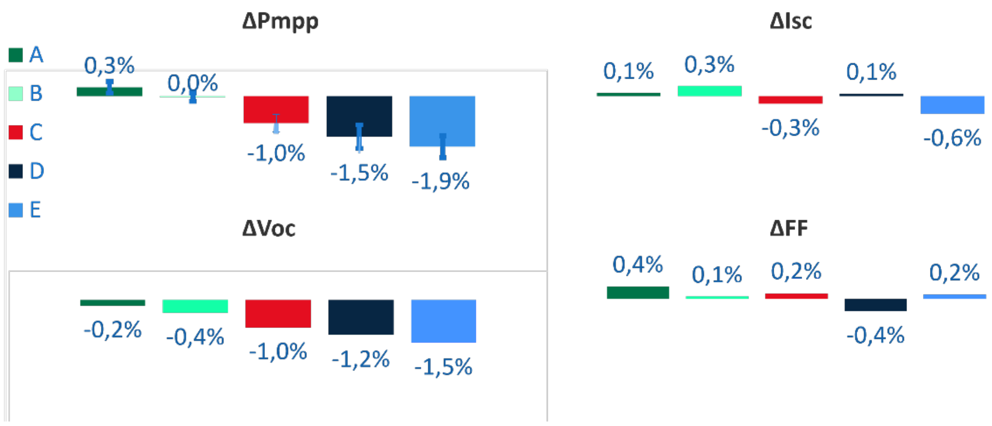

Figure 6. *Change in maximum power (ΔPmpp), open-circuit voltage (ΔVoc), short-circuit current (ΔIsc), and fill factor (ΔFF)—for TOPCon module types A, B, C, D, E after nine month of outdoor exposure.*

Module A shows a slight positive change in maximum power (ΔPmpp) (+0.3%), while Module B remains stable (0.0%). Modules C, D, and E exhibit significant power losses, increasing in magnitude from C (-1.0%) to D (-1.5%) and E (-1.9%). This trend suggests that Modules C–E are more prone to performance degradation under the tested conditions compared to A and B.

Modules of types A and B show minor decreases open-circuit voltage (ΔVoc) (average of -0.2% and -0.4%, respectively). Modules of type C, D, and E again demonstrate more pronounced losses, with average values of -1.0%, -1.2%, and -1.5%, respectively. The correlation between ΔPmpp and ΔVoc indicates that voltage degradation is a key contributor to power loss in these modules. Modules of type A and B show small positive changes in short-circuit current (ΔIsc) (average of +0.1% and +0.3%, respectively), while modules of type C remains nearly unchanged (average of +0.1%). Modules of type D and E exhibit slight decreases (average of -0.3% and -0.6%, respectively). These results suggest that short-circuit current is less affected by degradation mechanisms. The fill factors of modules of type A show a minor increase (average of +0.4%), while modules of type B, C, and E exhibit negligible changes (average of +0.1% to +0.2%). Modules of type D are the only one with a small negative change (-0.4% in average).

The data reveal that modules of type C, D, and E experience the most significant performance losses, particularly in maximum power (ΔPmpp) and open-circuit voltage (ΔVoc). Short-circuit current (ΔIsc) remains relatively stable across all module types, while the fill factor (ΔFF) shows minimal variation except for a slight decline in Module D. These results suggest that degradation mechanisms primarily affect voltage-dependent parameters, with varying susceptibility among module types.

The UV irradiation calculated for the field test duration using NASA data and taking the angle of incidence into account amounted to 68 kWh/m². However, the degradation observed under outdoor conditions is markedly lower than the values expected from laboratory UV tests (e.g., UV60). For instance, outdoor modules of type E show an average power degradation of −1.9% compared to −5.5% under laboratory conditions at UV60. For better comparability, the values are plotted side by side in Figure 7.

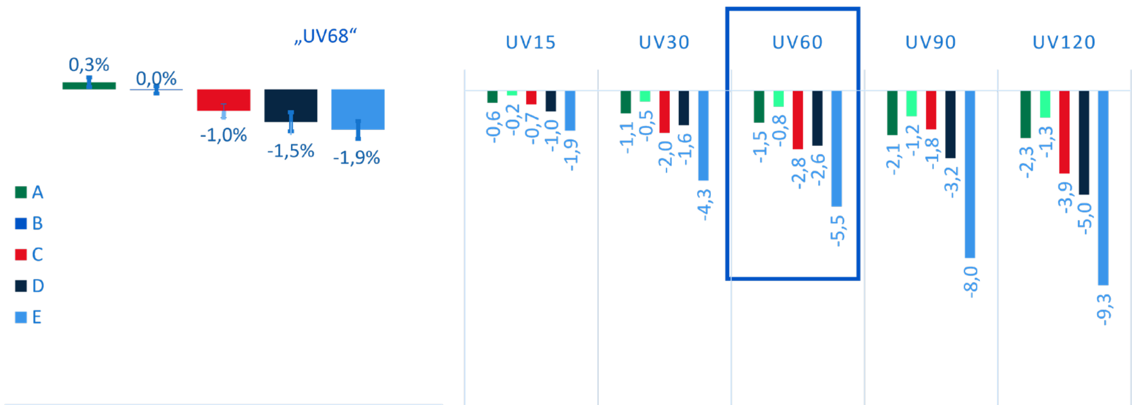

Figure 7. *Power degradation after field exposure (left side) and after UV exposure (right side) for modules types A – E.*

This discrepancy may indicate that outdoor conditions involve additional factors (e.g., temperature cycles or diffuse sunlight) that mitigate the effects of direct UV radiation observed in controlled lab environments.

The electroluminescence (EL) images of modules of types A – E after outdoor exposure are shown in Figure 8. The EL images for modules of type A and B show consistent brightness across all cells, indicating minimal degradation. This aligns with the power degradation shown in Figure 6, where these modules exhibit negligible changes in ΔPmpp (+0.3% for A, 0.0% for B). Modules of types C – E show noticeable dark regions in their EL images after outdoor exposure, indicating localized degradation. This corresponds to the average performance losses (ΔPmpp = −1.0%, −1.5%, −1.9% for modules of types C, D, and E, respectively).

For comparison, for each module type A – E, the EL images of a module without UV or outdoor exposure are shown (Figure 8, right side). The stored modules show no or only slight darkening, hinting that storage in the dark without UV or sunlight exposure does not lead to degradation.

The EL images visually confirm the trends observed in Figure 6. Modules A and B demonstrate high stability under outdoor conditions and storage, while Modules C–E show varying degrees of degradation that worsen during storage. The spatial heterogeneity of darkened regions highlights localized damage mechanisms affecting module performance parameters such as power output and voltage efficiency.

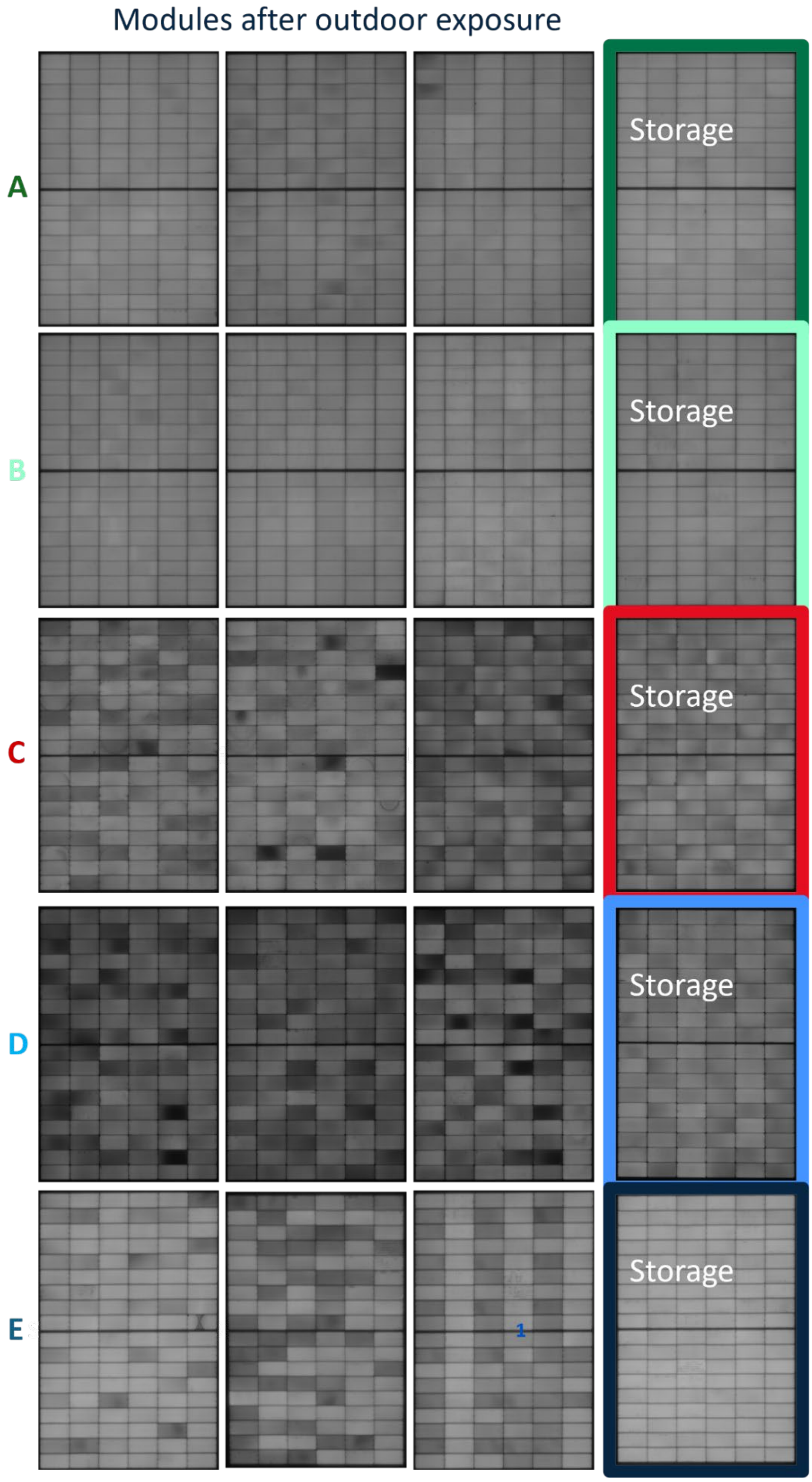

Figure 8. *Electroluminescence (EL) images of modules of types A – E after outdoor exposure.*

4. Conclusions

This study highlights the significant impact of ultraviolet-induced degradation (UVID) on TOPCon solar modules, with a strong dependency on the bill of materials (BOM). Laboratory tests revealed substantial power losses ranging from 1.3% to 13.7% after exposure to 120 kWh/m² of UV radiation, underscoring the variability in material resistance among different BOMs. Notably, additional degradation was observed beyond this UV dose, emphasizing the importance of prolonged exposure assessments. Additional degradation occurred during storage, which was partially reversible when the modules were re-irradiated.

In contrast, outdoor field tests showed lower degradation rates than expected from laboratory results. For instance, modules of type E exhibited a power loss of −1.9% after outdoor exposure, significantly less than the −5.5% observed under laboratory conditions at UV60. This discrepancy suggests that real-world environmental factors, such as temperature fluctuations and diffuse sunlight, may mitigate the effects of direct UV radiation observed in controlled lab settings. These findings emphasize the need for comprehensive testing that includes both laboratory and field conditions to accurately assess the long-term stability of TOPCon modules. It should be emphasized that due to the small number of modules examined, the statistical significance of the study is limited. Nevertheless, the results provide evidence of UV degradation under field conditions. The results highlight the importance of material selection and quality control in module manufacturing.

To prevent or at least reduce UV degradation of TOPCon modules, the quality of the AlOx layer, as well as the thickness, refractive index, and homogeneity of the SiN layer should be ensured in solar cell production, and the UV stability of solar cells should be randomly checked in the incoming inspection of module production. If this is not possible, the use of UV blockers in the front encapsulation foil should be considered.

Author contributions

Conceptualization: Sandra Lust, Lars Podlowski

Project administration, investigation: Shiva Ram Kuntamukkula, Sören Friedrichs

Data curation, writing – review & editing: Shiva Ram Kuntamukkula

Validation, visualization, writing – original draft: Sandra Lust

Competing interests

The authors declare that they have no competing interests.

Funding

This work was supported by the German Federal Ministry for Economic Affairs and Energy (BMWi) under the contract number 03EE1112D, acronym EVAplus.

Acknowledgement

We would like to thank Nattapark Pongthanacharoenkul and Alexander Preiss for providing the UV data.

References

[1] M. Köntges , J. Lin , A. Virtuani, G. C. Eder, G. Oreski, P. Hacke, J. S. Stein, L. Bruckman, P. Gebhardt, D. Barrit, M. Rasmussen, I. Martin, K. O. Davis, G. Cattaneo, B. Hoex, Z. Hameiri, E. Özkala. „Degradation and Failure Modes in New Photovoltaic Cell and Module Technologies". Report IEA-PVPS T13-30:2025 2025 doi: https://doi.org/10.69766/ATBD2730. (accessed 05.03.2025).

[2] F. T. Thome, P. Meßmer, S. Mack, E. Schnabel, F. Schindler, W. Kwapil, M. C. Schubert. "UV-Induced Degradation of Industrial PERC, TOPCon, and HJT Solar Cells: The Next Big Reliability Challenge?" Sol. RRL 2024 **8** 2400628. doi: https://doi.org/10.1002/solr.202400628.

[3] P. Gebhardt. "Reliability of Commercial TOPCon PV Modules An Extensive Comparative Study". PVSEC Wien 2024.

[4] M. U. Khan, C. Sen, M. Pollard, Y. Wu, R. X. Wu, H. Wang, X. Wang, G. Zhang, B. Hoex . "Shedding a light on UV induced degradation of TOPCon solar cells." PVSEC Wien 2024

[5] Sinha, J. Qian, S. L. Moffitt , K. Hurst, K. Terwilliger, D. C. Miller, L. T. Schelhas, P. Hacke. „UV-induced degradation of high-efficiency silicon PV modules with different cell architectures." Prog in Photovolt. 2023 **31** (1) 36–51.

[6] R. Witteck, B. Min, H. Schulte-Huxel, H. Holst, B. Veith-Wolf, F. Kiefer, M. R. Vogt, M. Köntges, R. Peibst, R. Brendel. „UV radiation hardness of photovoltaic modules featuring crystalline Si solar cells with AlOx/p+-type Si and SiNy/n+-type Si interfaces." Phys. Stat. sol. RRL. 2017 **11** (8) 1700178. doi: https://doi.org/10.1002/solr.202400628.

[7] J. Schmidt, B. Hoex. „*Verfahren zum Herstellen einer Solarzelle mit einer oberflächenpassivierenden Dielektrikumdoppelschicht und entsprechende Solarzelle*." Europäische Patentschrift 2007 EP 2 220 689 B1